applied sciences

MDPI

Article

Sulfonated Polyethersulfone Membranes for Brackish Water Desalination: Fabrication, Characterization, and Electrodialysis Performance Evaluation

Li Chen [1,2], Eva M. Deemer [3,*], XiuJun Li [4,*] and W. Shane Walker [5,*]

[1] Center for Inland Desalination System (CIDS), The University of Texas at El Paso, 500 W. University Ave., El Paso, TX 79968, USA; li.chen20111021@gmail.com
[2] Nanotechnology-Enabled Water Treatment (NEWT), Engineering Research Center (ERC), Rice University, 6100 Main St., MS 6398, Houston, TX 77005, USA
[3] Environmental & Occupational Health Sciences, School of Public Health in El Paso, University of Texas Health Science Center at Houston, 5130 Gateway Boulevard East, El Paso, TX 79905, USA
[4] Department of Chemistry and Biochemistry, The University of Texas at El Paso, 500 W. University Ave., El Paso, TX 79968, USA
[5] Department of Civil, Environmental, and Construction Engineering, Water and the Environment Research (WATER) Center, Texas Tech University, 2500 Broadway W, Lubbock, TX 79409, USA
* Correspondence: eva.deemer@uth.tmc.edu (E.M.D.); xli4@utep.edu (X.L.); shane.walker@ttu.edu (W.S.W.)

Abstract: The widespread application of electrodialysis is constrained by the high cost of ion exchange membranes, necessitating the development of affordable alternatives. This study focuses on the fabrication and performance evaluation of cation exchange membranes made from polyethersulfone (PES) and sulfonated polyethersulfone (sPES). Membranes were synthesized through phase inversion with varying solvent evaporation times, using N-Methyl-2-Pyrrolidone (NMP) as the solvent. The structural and functional modifications were confirmed using FTIR, XPS, and AFM techniques. Performance tests identified optimal electrodialysis results for PES membranes with a 3 h solvent evaporation time and for sPES membranes with a 1 h evaporation time. Under varying operational conditions, including applied voltage, flow rates, and feed solutions, sPES membranes demonstrated superior performance, underscoring their potential for cost-effective brackish water desalination applications.

Keywords: electrodialysis; desalination; ion exchange membrane; polyethersulfone; sulfonation; real brackish water; membrane selectivity

Academic Editor: Andrei Sarbu

Received: 13 November 2024
Revised: 6 December 2024
Accepted: 20 December 2024
Published: 30 December 2024

Citation: Chen, L.; Deemer, E.M.; Li, X.; Walker, W.S. Sulfonated Polyethersulfone Membranes for Brackish Water Desalination: Fabrication, Characterization, and Electrodialysis Performance Evaluation. *Appl. Sci.* **2025**, *15*, 216. https://doi.org/10.3390/app15010216

1. Introduction

Water scarcity is a critical challenge for human society. Besides surface water and fresh groundwater, brackish groundwater is another crucial source of water supply. However, it is necessary to remove salt from brackish groundwater or other saline water to make it drinkable. Desalination, especially from brackish water sources, plays a vital role in augmenting freshwater supplies. While reverse osmosis (RO) dominates the desalination industry, electrodialysis (ED) has garnered increasing attention due to its faster kinetics, solute-solute selectivity, and ability to recover valuable ions from diverse feed streams like brackish water [1]. These merits make ED particularly suitable for resource recovery and specialized desalination applications.

Recent studies further highlight the growing interest in ED for its distinct advantages over RO. For instance, ED offers the ability to recover valuable ions directly during desalination, making it highly efficient in processes such as brine management and metal

recovery. Latinis et al. (2021) demonstrated how optimal operational profiles in ED units can enable efficient ion recovery, especially for applications requiring high-value material recovery [2]. Additionally, Juve et al. (2022) reviewed ED's capabilities for selective removal and recovery of metals, underscoring its potential in wastewater treatment and industrial process streams [3]. This feature not only contributes to resource recovery but also reduces the environmental impact of desalination by minimizing waste.

Moreover, ED systems are characterized by faster desalination kinetics compared to pressure-driven processes like RO. The direct migration of ions under an electric field significantly reduces energy requirements for brackish water desalination [4]. Unlike RO, which relies on high-pressure membranes, ED can operate at lower pressures and is less prone to fouling and scaling. This reduces maintenance requirements and operational costs, particularly in industrial applications with varying water quality. Furthermore, the selective ion transport capability of ED enables it to separate specific ions, which is advantageous for specialized desalination needs or the production of tailored water compositions.

To enable efficient ion transport and separation in electrodialysis (ED), a variety of ion exchange membranes (IEMs) based on different materials have been developed, each offering distinct advantages and limitations. Sulfonated poly(ether ether ketone) (SPEEK) membranes are widely utilized due to their high thermal stability, chemical resistance, and tunable ion exchange capacity. These properties make them suitable for harsh desalination conditions, as demonstrated by their improved proton exchange performance when doped with ionic liquids, enhancing conductivity and selectivity [5]. Polyethersulfone (PES) membranes, particularly when sulfonated, exhibit good mechanical strength and chemical durability, making them a common choice for cost-effective ED applications [6]. Similarly, polyvinylidene fluoride (PVDF) has garnered attention as a robust base material, offering excellent chemical resistance and stability. PVDF membranes, when modified to include cation exchange functionalities, have shown improved performance in ED by optimizing crystallinity and mitigating co-ion leakage [7].

Polystyrene-based membranes, functionalized with sulfonic or quaternary ammonium groups, are another prevalent material due to their high ion exchange capacity and ease of fabrication. However, their performance can be enhanced further with radiation-induced grafting, as demonstrated by Golubenko et al., who achieved superior performance for reverse electrodialysis applications [8]. Additionally, polyamide-based membranes are emerging as promising alternatives for cation-selective transport. These membranes, traditionally used in reverse osmosis, have demonstrated high selectivity and durability in electrodialysis, enabling efficient ion transport while maintaining chemical stability [9].

Recent developments in ED membrane technology have led to promising innovations, including the incorporation of advanced materials such as metal–organic frameworks (MOFs) for enhanced efficiency and nanoparticles for improved ion selectivity. Despite these achievements, many approaches face challenges due to complex synthesis methods, high costs, and limited scalability. For instance, Zhao et al. developed cation exchange membranes using poly(p-phenylene terephthalamide) (PPTA) nanofibers and 2,5-diaminobenzenesulfonic acid (DSA), which demonstrated exceptional thermal stability, solvent resistance, and ion exchange capacity. However, this method required intricate fabrication processes, producing membranes with a salt removal rate of 95–99% for Na_2SO_4 and $(NH_4)_2SO_4$ over 220 min, at a current density of ~32 mA/cm^2 [10].

Similarly, Khan et al. reported anion exchange membranes fabricated with brominated poly(2,6-dimethyl-1,4-phenylene oxide) (BPPO) and dimethylethanolamine (DMEA), achieving an impressive ion exchange capacity (1.38 mmol/g) and low resistance (1.43 $\Omega \cdot cm^2$). Despite their effectiveness in removing 80% of conductivity after 100 min, the process involved significant complexity in chemical handling [11]. Gahlot et al. further

explored zinc MOFs combined with sulfonated polyethersulfone (sPES) to create composite membranes, achieving a 94.1% salt removal rate in 200 min and low energy consumption (1.02 kWh/kg salt removed). However, such methods also require precise material handling and multi-step synthesis [12].

He et al. demonstrated the scalability of sulfonated poly(ether ether ketone) (SPEEK) membranes, which achieved 67.6% salt removal with notable current efficiency (78.2%) [13]. Additionally, Wu et al. introduced sub-nanoporous polyethersulfone membranes with excellent ion separation selectivity (e.g., K^+: Na^+: Li^+: Mg^{2+} ratios of 83:56:14:1 for 10 min under UV sensitization) [14]. However, their industrial applicability remains constrained by scalability challenges. Other studies have explored enhancing ion-exchange membranes with nanoparticles. Zhu et al. achieved improved antibacterial properties and desalting performance with silver nanoparticle modifications (NaCl removal ratio of 67.5%, current efficiency of 96.9%) [15]. Meanwhile, Gahlot et al. reported nearly complete salt removal (99.1%) and high efficiency (97.4%) with graphene oxide nanocomposites [16]. Fan et al. developed asymmetric cation exchange membranes, demonstrating a salinity reduction rate of 91.9% and energy efficiency of 127.5% [17]. However, in spite of these performance enhancements, the integration of nanoparticles into membranes presents challenges, including complex synthesis processes and material handling difficulties, which hinder large-scale industrial application.

To address these challenges, this work focuses on the development of ion exchange membranes using simple polyethersulfone (PES) and sulfonated PES (sPES). The straightforward fabrication process involves phase inversion, avoiding the need for complex additives or multistep synthesis. This approach aims to provide cost-effective, high-performance membranes suitable for brackish water desalination applications.

2. Materials and Methods

2.1. Materials

Polyethersulfone (PES) was obtained from Goodfellow (SU30-GL-000111, nominal granule size 3 mm, molecular weight 58,000 g/mol, melt volume rate: 35 cc/10 min at 360 °C, Pittsburgh, PA, USA). Dichloromethane (DCM, CH_2Cl_2), an ACS-grade solvent (VWR BDH, Radnor, PA, USA), was utilized for PES sulfonation. Chlorosulfonic acid (CSA, HSO_3Cl, >98.0%, Honeywell Fluka, Charlotte, NC, USA) served as the sulfonating agent, while N-Methyl-2-pyrrolidone (NMP, C_5H_9NO), another ACS-grade reagent (Fisher Scientific, Hampton, NH, USA), was used to prepare the solvent for membrane fabrication. Membranes were cast using Petri dishes. Sodium chloride (NaCl) and sodium sulfate (Na_2SO_4), both laboratory-grade (ACS reagent grade), were purchased from Fisher Scientific (USA) for preparing feed and electrode rinse solutions. Unless stated otherwise, all electrodialysis (ED) experiments were conducted in triplicate.

2.2. Fabrication of PES and sPES Membranes

2.2.1. Fabrication of PES Membranes

The fabrication diagram of PES cation exchange membranes is shown in Figure 1. Firstly, 30 g of PES pellets were weighed and dissolved into 170 g NMP solvent, making 200 g PES dope solution for subsequent use. Secondly, 2.0 g PES dope solution was cast into each Petri dish and left at room temperature to evaporate for 0.5 h, 1 h, 2 h, 3 h, 4 h, 8 h,16 h, and 24 h, respectively. Then, those Petri dishes were submerged in DI water to form the PES membranes through the phase inversion effect.

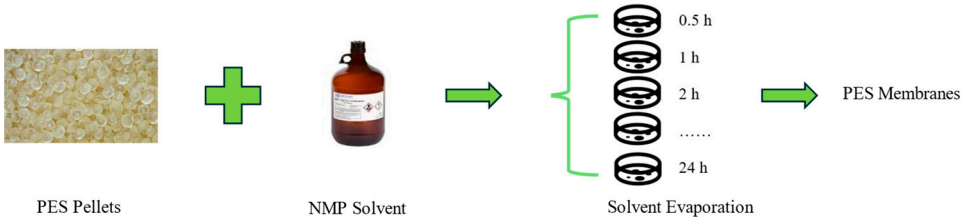

Figure 1. Conceptual process of PES membrane fabrication.

2.2.2. Fabrication of sPES Membranes

The general fabrication diagram of sPES cation exchange membranes is shown in Figure 2a. The first step was sulfonation by CSA [18–21]. As shown in Figure 2b, the sulfonation process would increase the content of the HO_3S^- group. Specifically, blank PES (bPES) weighed 30 g and was dissolved into 150 mL DCM. Then, 8 mL CSA was added, and the mixture was stirred for 60 min. The mixture was quenched with 300 mL methanol. The phase inversion method was applied to solidify sulfonated PES (sPES) by adding 170 g NMP to form sPES solution and slowly pouring sPES/NMP solution into DI to form sPES noodles. The noodles soaked for over 24 h to neutralize pH. The process was repeated three times to thoroughly neutralize pH. The solid sPES material was removed and placed under the fume hood to fully dry for subsequent use. In addition to the sulfonation dose of 8 mL CSA, greater degrees of sulfonation were attempted with doses of 16 mL and 24 mL CSA. However, the sPES cannot form a membrane with 24 mL CSA after purification. Also, with 16 mL CSA, the formed sPES membranes were fragile in mechanical strength, which meant they were fragile and easily broken. Thus, the sulfonation method with 8 mL CSA was chosen for the following experiments.

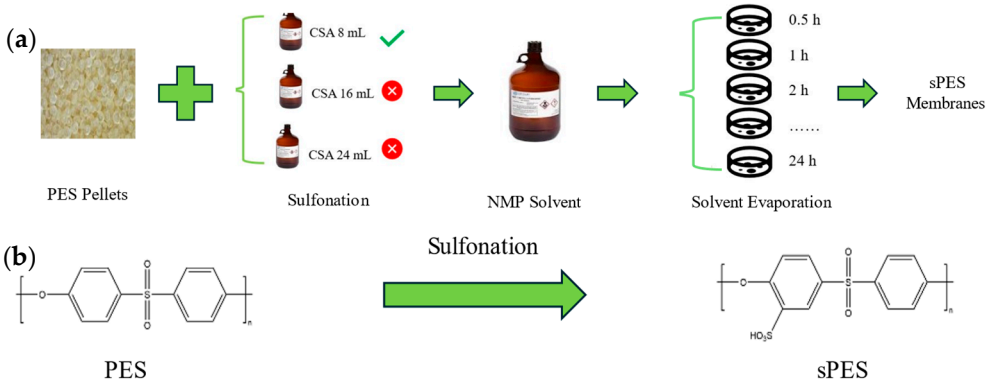

Figure 2. (**a**) Conceptual process of sPES membrane fabrication. (**b**) Molecular modification of PES polymer to sPES polymer.

After the dry sPES material was produced, the second step was identical to the fabrication process of PES membranes. The sPES dope solution was made for the membrane's fabrication process. Firstly, 30 g sPES was weighed and put into 170 g NMP to make a 15% sPES dope solution. Secondly, 2.0 g sPES dope solution was cast into each petri dish and put in the air to evaporate for 0.5 h, 1 h, 4 h, 8 h, 12 h, 16 h, 20 h, and 24 h, respectively, then they were submerged in DI water to form the sPES membranes.

2.3. Characterization of PES and sPES Membranes

2.3.1. Degree of Sulfonation (DS) Measurements

The degree of sulfonation (*DS*) is the fraction of the sulfonated monomer units after the reaction. Membranes were dried and weighed, then soaked in 2 M NaCl solution for 24 h to release the sulfonic acid groups into the solution. Next, sodium hydroxide with

a concentration of 0.1 M was titrated into the mixture. Phenolphthalein was used as an indicator. The following formula (Equation (1)) was used for the calculation of *DS* [22–24]:

$$DS = \frac{244\ \text{g/mol}(C_{\text{NaOH}} \times V_{\text{NaOH}})}{W - 81\text{g/mol}(C_{\text{NaOH}} \times V_{\text{NaOH}})} \quad (1)$$

where C_{NaOH}, V_{NaOH}, and W represent the concentration (mol/L) of the standard NaOH solution, the volume (mL) of NaOH solution used during neutralization, and the weight (g) of the dry ion exchange membranes (IEMs), respectively. The molecular weight of the PES repeating unit is 244 g/mol, while the sulfonate group (SO_3H) has a molar mass of 81 g/mol.

2.3.2. Ion-Exchange Capacity (IEC) Measurements

Ion-exchange capacity (*IEC*) quantifies a material's ability to exchange ions embedded within its structure. For this measurement, the membranes were first immersed in 1 M HCl for 24 h, followed by rinsing with deionized water to eliminate surface acid residues. They were then transferred to a 2 M NaCl solution for another 24 h. Afterward, the solution was titrated with NaOH, using phenolphthalein as an indicator. The *IEC*, expressed in milliequivalents per gram (meq/g), was determined using the formula provided in Equation (2) [24,25]:

$$IEC = \frac{C_{\text{NaOH}} \times V_{\text{NaOH}}}{W_{\text{Dry}}} \quad (2)$$

where C_{NaOH}, V_{NaOH}, and W_{Dry} denote the concentration (eq/L) of the standard NaOH solution, the volume (mL) of NaOH solution utilized for neutralization, and the weight (g) of the dry ion exchange membranes (IEMs), respectively.

2.3.3. Fourier Transform Infrared-Attenuated Total Reflectance (FTIR-ATR) Measurements

Fourier transform infrared (FTIR-ATR) analysis was performed using a Nicolet™ iS™ 5 FTIR instrument with an iD7 attenuated total reflectance (ATR) diamond accessory (Thermo Fisher Scientific, Waltham, MA, USA). All FTIR-ATR data sets were normalized by dividing the signal output by the intensity of the greatest peak value in the series.

2.3.4. Atomic Force Microscopy (AFM) Measurements

AFM was utilized for material characterization analyses primarily due to its capability to provide high-resolution imaging at the atomic or molecular level. This is essential for understanding the surface structure and properties of materials. One of the key advantages of AFM is its non-destructive nature, meaning it does not alter or damage the sample under study, which is crucial for delicate or expensive materials. The data from the photodetector are processed to generate a detailed map of the surface topography and properties.

In this study, AFM measurements were conducted using a standard commercial tip (DNP-S10-B, Bruker, Camarillo, CA, USA) with a spring constant of 0.12 N/m. Images were captured in ambient air under tapping mode and digitized at a resolution of 512 × 512 pixels. Multiple scans were performed at randomly selected areas of the film surface to ensure comprehensive analysis. The obtained topographic image data were then converted into ASCII format for further processing and evaluation.

2.3.5. X-Ray Photoelectron Spectroscopy (XPS) Measurements

XPS (Nexsa G2, Thermo Scientific, Waltham, MA, USA) was used for material characterization analysis, primarily for its ability to provide detailed information about the elemental composition, chemical states, and electronic states of materials at the surface level.

This surface sensitivity, typically up to 10 nm deep, makes XPS invaluable for studying thin films, coatings, surface treatments, and interfaces in a range of materials.

2.4. Electrodialysis Desalination Performance Testing

A batch-cycle ED system was assembled with a pump (Cole-Parmer. Vernon Hills, IL, USA, Model: 7519-00), one-liter stream reservoirs stirred by non-heating magnetic stirrers (Fisher Scientific, Waltham, MA, USA, model: Fisher 14-955-150), two pH/conductivity meters (Thermo Scientific, Bartleville, OK, USA, model: Orion Star A325), a digital scale (Meller Toledo, Columbus, OH, USA, model: XS2002S), a programmable DC power supply (B&K Precision, Yorba Linda, CA, USA, Model: 9123A), and a MicroED stack (PCCell/PCA, GmbH, Heusweiler, Germany, model: 08002-001). The active cross-sectional area of membranes assembled in the micro-ED was 7.48 cm^2 (2.8 cm $\times$ 2.8 cm). The thickness of the polyester spacer was 0.45 mm used to separate the AEMs and CEMs [26].

The feed water used was a 3.0 g/L NaCl solution. The flow velocity of the diluate stream was maintained at 3 cm/s, and the stack voltage was set to 0.8 V per cell pair. The membrane combinations tested included PES with Neosepta AMX76 (ASTOM, Tokyo, Japan), and sPES with Neosepta AMX76.

3. Results and Discussions

3.1. Examples of Fabricated Membranes

Examples of selected cast PES membranes with 1 h, 4 h, 8 h, and 24 h solvent evaporation times are shown in Figure 3a. These time points were chosen because salinity reduction performance of PES membranes significantly decreases beyond 8 h, making longer evaporation durations less practical. As shown in the figure, the PES membrane with 1 h solvent evaporation time has no transparency, but with the increase of solvent evaporation time, the PES becomes more translucent. When the time reaches 24 h, the PES becomes transparent. For sPES membranes, examples with 0.5 h, 8 h, 16 h, and 24 h evaporation times are shown in Figure 3b, reflecting their extended performance up to 20 h, with an even distribution of selected times for comparison. From the figure, 0.5 h sPES has no transparency. With the increased solvent evaporation time, the sPES membranes become more translucent. When the time reaches 24 h, the sPES membranes become transparent.

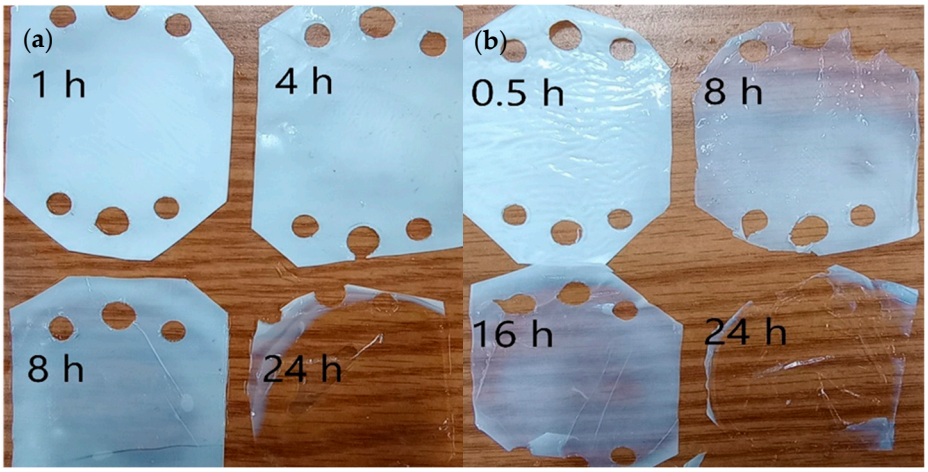

Figure 3. (**a**) PES membrane examples with 1 h, 4 h, 8 h, and 24 h solvent evaporation time. (**b**) sPES membrane examples with 0.5 h, 8 h, 16 h, and 24 h solvent evaporation time.

Both membranes exhibited a similar trend of becoming more translucent with the increase of the solvent evaporation time but with a slightly different timeline. As time increased within 24 h, the sPES membranes progressively became more translucent. The

differences in the intermediate transparency stages between PES and sPES membranes might be attributed to the distinct chemical and physical properties of the base polymers, that after sulfonation, the sPES membranes may have a more open or porous structure facilitating faster solvent evaporation. However, transparency is an indication of excessive density, which while enhancing mechanical stability, inhibits ion exchange and diminishes salinity reduction performance, making such membranes unsuitable for electrodialysis applications.

3.2. Membrane Fabrication Condition Optimization

Based on different solvent evaporation times (0.5 h, 1 h, 2 h, 3 h, 4 h, 8 h, 16 h, and 24 h), different PES membranes were fabricated. Testing results were generated to optimize the fabrication based on running conditions, like 3 g/L NaCl feed solution, 3 cm/s flow velocity, and 0.8 v/cell-pair. As shown in Figure 4a, with solvent evaporation times from 0 to 3 h, the current density increased due to decreasing electrical resistance of the membrane. When the solvent evaporation time was 3 h, the current density of PES exhibited the best performance, which was 97 A/m^2. Furthermore, when the solvent evaporation time increased beyond 3 h, the current density decreased, possibly due to increasing membrane density. After 8 h evaporation time, the current density decreased to 10 A/m^2.

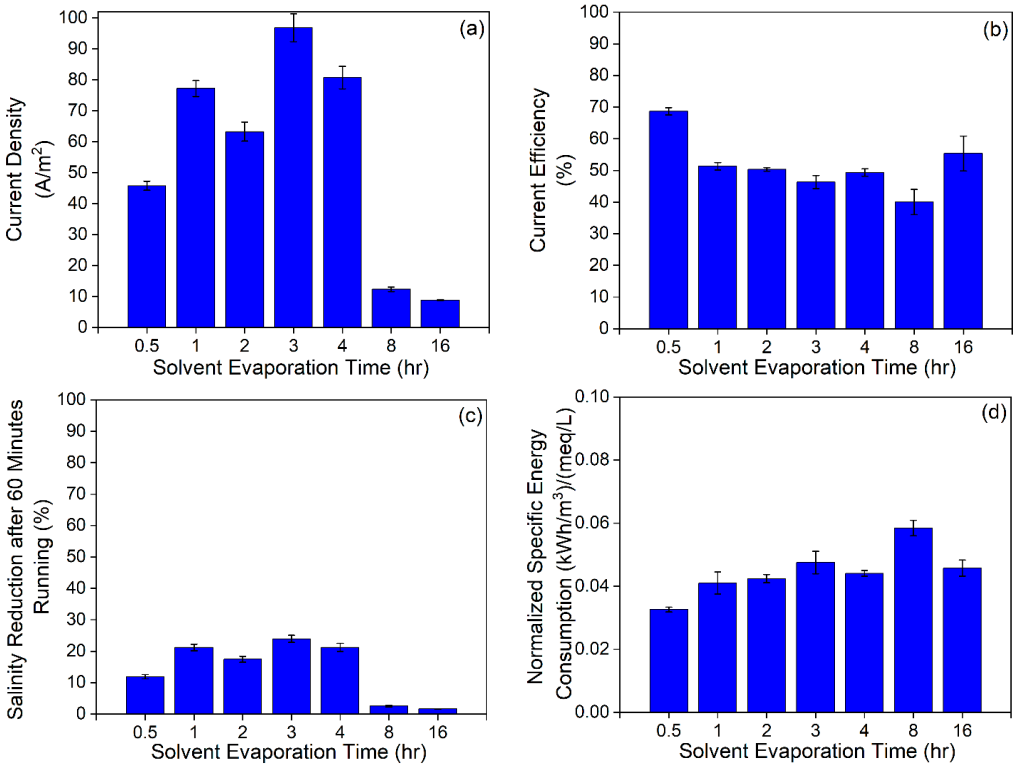

Figure 4. ED performance results of PES membranes in different solvent evaporation times: (**a**) current density (CD), (**b**) current efficiency (CE), (**c**) salinity reduction (SR) after 60 min running, and (**d**) normalized specific energy consumption (nSEC).

As shown in Figure 4b, when the solvent evaporation time was 0.5 h, the current efficiency of PES showed the best performance at 69%. However, most of the PES membranes showed a current efficiency of nearly 50%, implying that approximately 50% of the electricity was used to remove salts. As shown in Figure 4c, the best performance of salinity reduction after 60 min occurred when the PES solvent evaporation time was 3 h (24% removal). Starting from 8 h solvent evaporation time, the salinity reduction performance decreased substantially. As shown in Figure 4d, most PES membranes showed

a normalized specific energy consumption range of 0.040–0.050 kWh/m^3 per meq/L of salinity removed.

Based on different solvent evaporation times (0.5 h, 1 h, 4 h, 8 h, 12 h, 16 h, 20 h, and 24 h), different sPES membranes were fabricated. Moreover, testing results were generated to optimize the fabrication based on preliminary running conditions, like 3 g/L NaCl feed solution, 3 cm/s flow velocity, and 0.8 v/cell-pair. As shown in Figure 5a, when the solvent evaporation time was within 1 h, the current density of sPES showed the best performance, which was 130 A/m^2. Moreover, when the solvent evaporation time increased, the current density decreased gradually. Starting from 24 h, the current density decreased obviously, and the lowest was 10 A/m^2 when the solvent evaporation time was 24 h. From 20 h, the current density decreased obviously, which meant the membrane resistance increased obviously. It was probably because of the membrane becoming denser, the porosity becoming small, and no porosity stopping ions from passing through [27,28]. Compared with the current density of PES membranes, the changes of current density of sPES membranes were much smaller; this indicated that the sulfonation process significantly decreased the influence of solvent evaporation.

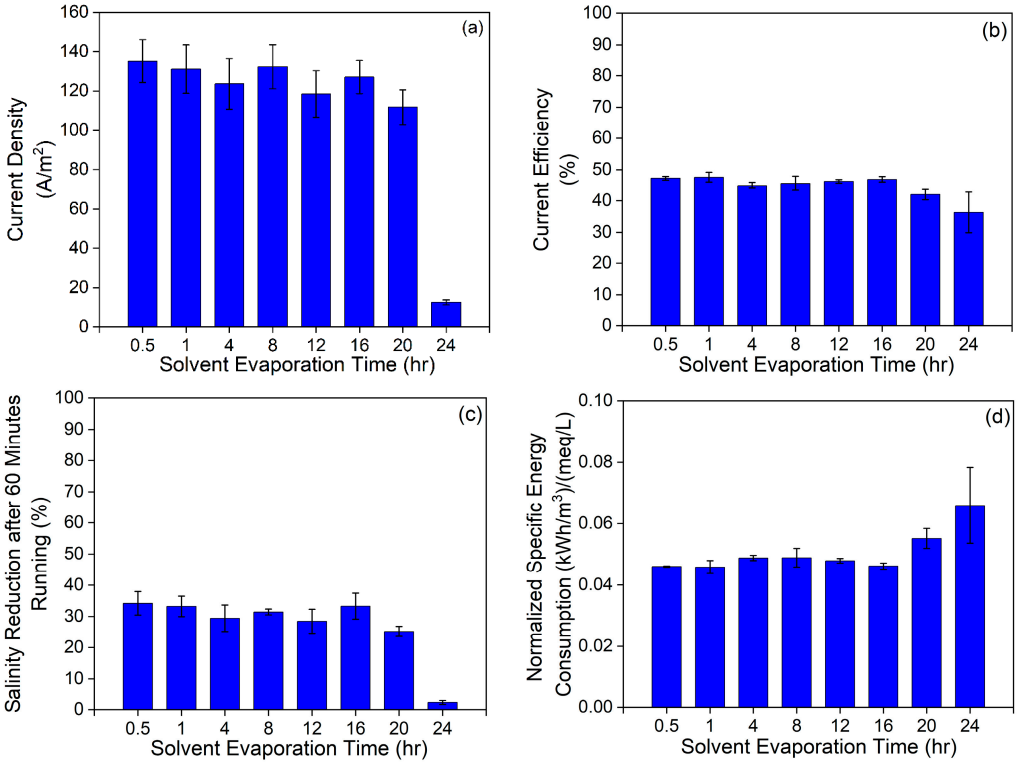

Figure 5. ED performance results of sPES membranes in different solvent evaporation times: (**a**) current density (CD), (**b**) current efficiency (CE), (**c**) salinity reduction (SR) after 60 min running, and (**d**) normalized specific energy consumption (nSEC).

As shown in Figure 5b, most of the sPES membranes showed a current efficiency of 48%, which meant that 48% of the electricity was used to remove salts. In addition, starting from 24 h solvation evaporation time, the current efficiency performance decreased substantially. Compared with the PES membranes, while the current density of the sPES membranes was higher, the current efficiency of sPES membranes was slightly lower than that of the PES membranes. These results indicated that the higher current density did not have effects on current efficiency. With more ions passing through sPES membranes, there may be more co-ions passing through sPES membranes too, which resulted in slightly lower current efficiency. As shown in Figure 5c, when the solvent evaporation time was

within 1 h, the salinity reduction after 60 min of running sPES membranes showed the best performance, which was 33%. Starting from 20 h, the salinity reduction performance decreased substantially. As shown in Figure 5d, when the solvent evaporation time was within 1 h, the normalized specific energy consumption of sPES exhibited the best performance, which was 0.045 kWh/m^3 per meq/L of salt removed. Moreover, starting from 20 h, the normalized specific energy consumption performance increased substantially.

Based on the results shown in Figure 4, it can be concluded that for PES membranes, when the solvent evaporation time was 3 h, the general performance of the PES membrane was the best. For sPES membranes, as shown in Figure 5, when the solvent evaporation time was within 1 h, the general performance of the sPES membrane was the best. Therefore, PES membranes and sPES membranes with the best performance were chosen for future analysis, which meant PES membranes with a solvent evaporation time of 3 h and sPES membranes with a solvent evaporation time of 1 h were selected for subsequent evaluations.

3.3. Membrane Characterization

This section presents the analysis of Fourier Transform Infrared Spectroscopy with Attenuated Total Reflectance (FTIR-ATR), X-ray Photoelectron Spectroscopy (XPS), and Atomic Force Microscopy (AFM) to elucidate the structural and surface differences between the PES and sPES membranes.

The FTIR-ATR spectra of PES and sPES membranes are shown in Figure 6. The absorption peak at 1010 cm^{-1} is characteristic of the aromatic -SO_3H symmetric stretching vibrations [29]. The normalized intensity of sPES is slightly stronger than that of PES, suggesting the introduction of sulfonic acid groups into the polymer chains. Additional characterization techniques are necessary to confirm this observation.

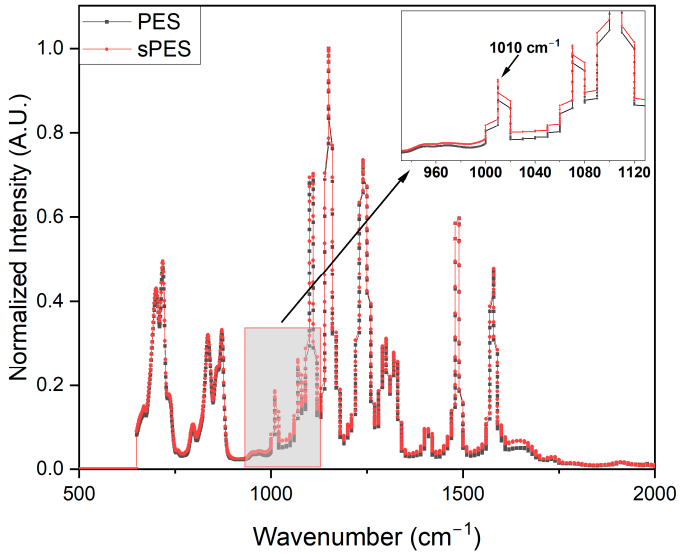

Figure 6. FTIR-ATR spectra of selected PES and sPES membranes.

XPS is essential for providing detailed information on the surface chemistry of membranes, particularly for identifying specific functional groups. Figure 7 presents the XPS spectra of PES and sPES membranes. The peak at 168 eV is characteristic of S2p, which indicates the existence of -SO_3H [17], providing evidence of the sulfonation process. From the XPS spectra, the peak of the sulfonic acid group of sPES is slightly stronger than that of PES. This enhancement can be attributed to the sulfonation process of sPES membranes, which incorporate more sulfonic acid groups into the polymer chains. Although the differences in peak intensities between PES and sPES are subtle, they align with the FTIR results,

collectively demonstrating the successful incorporation of sulfonic acid groups into the sPES polymer matrix.

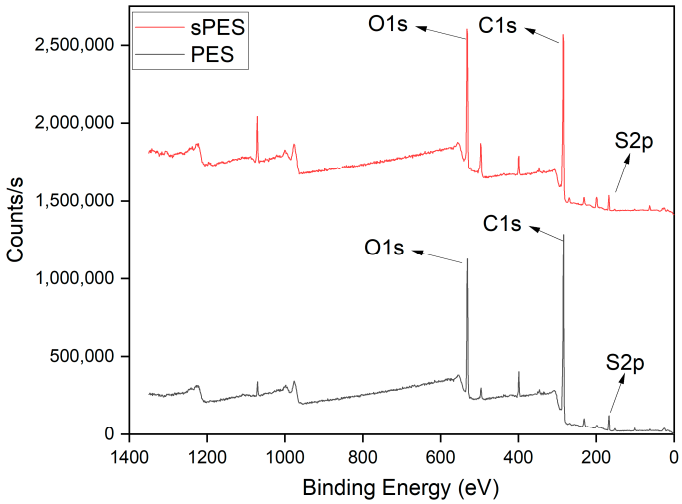

Figure 7. XPS spectra of selected PES and sPES membranes.

The surface morphologies of the PES and sPES characterized by AFM are shown in Figure 8. Surface changes reflect the influence that sulfonation has on the membrane morphology and can be observed by difference in the mean roughness (Ra). Consistent with previous research findings, the Ra parameters increased from PES (0.996 nm) to sPES (3.149 nm) with an increase in the sulfonation in the casting solution [30]. For PES, a relatively flatter smooth-phase morphology can be observed, while the sPES membranes exhibit more cluster-like features.

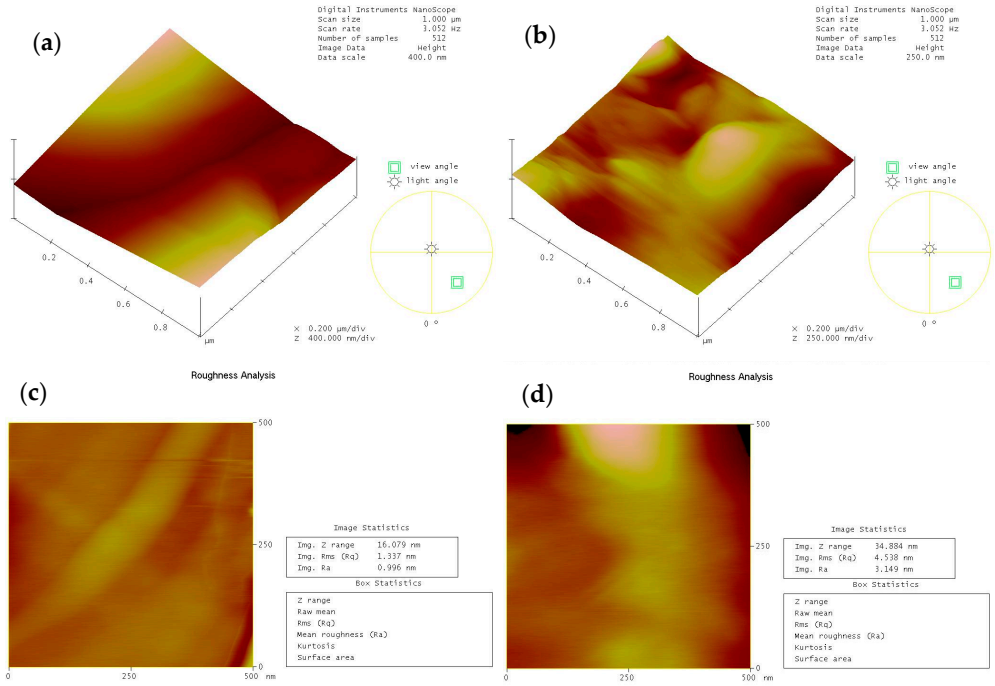

Figure 8. AFM figures of selected PES and sPES membranes: 1 µm × 1 µm AFM images of (**a**) PES and (**b**) sPES; 0.5 µm × 0.5 µm surface roughness analysis of (**c**) PES and (**d**) sPES.

3.4. Performance Testing

As shown in Table 1, according to Equations (1) and (2), the ion exchange capacity of the best PES membrane was 1.5 meq/g, and the corresponding sulfonation degree was

42%. The ion exchange capacity of the best sPES membrane was 2.67 meq/g, and the corresponding sulfonation degree was 83%.

Table 1. Ion exchange capacity and sulfonation degree of selected PES and sPES membranes.

	IEC (meq/g)	SD (%)
PES	1.5	42
sPES	2.67	83

More comparisons are shown in Table 2. As shown in Table 2, although there have been many IEMs developed by researchers for ED applications, most of them were fabricated with multiple materials, non-trivial physical or chemical treatments, or crosslinked with some other materials, making the fabrication process complicated or not cost-effective. In contrast, the membranes developed in this work demonstrate competitive performance with simpler, more scalable methods.

Table 2. Summary of IEMs developed for ED applications.

Sample	Membrane Material	IEC (meq/g)	CE (%)	Salt Removal (%)	Feed Solution (mol/L)	Reference
PDP-2.0	PPTA/DS/PPTA	1.6	-	95.1	0.08 Na_2SO_4	[10]
60SPSF-C2	SPSF/Acrylic crosslinker	1.6	95.7	91.7	0.1 NaCl	[11]
Z-2	Zn-MOF/sPES	-	75.8	94.1	0.1 NaCl	[12]
SPEEK/PGO-8	SPPEK/PGO	2.16	78.2	67.6	0.7 NaCl	[13]
Sub-nanoporous PES	PES	-	-	-	0.1 LiCl, NaCl, KCl, $MgCl_2$	[14]
SPSU-60	SPSF/AgNP	1.55	96.9	67.5	0.5 NaCl	[15]
SG-10	sPES/GO	1.27	97.4	99.1	0.1 NaCl	[16]
40% sPES-PES	sPES/PES/PVP	0.52	127.5	91.9	0.1 NaCl	[17]
S/P/PANi-0.6	sPES/PVP/PANi	0.47	94.3	-	0.1 NaCl	[31]
PAN-PAMPS-2	PAN/PAMPS	1.65	91	-	0.35 NaCl	[32]
DES-5	sPES/S-MoS2	1.42	69.5	-	0.1 NaCl	[33]
PVA/BFC-70	PVA/DVB/AMPS	1.3	87.5	-	0.85 NaCl	[34]
SPI/PGO-8	SPI/PGO	2.37	76.4	-	0.1 NaCl	[35]
SPK/IGO-8	SPEEK/IGO	2.23	82.9	-	0.85 NaCl	[36]
SGO-5	sPES/SGO	1.7	93.1	-	0.1 NaCl	[37]
S-25/P	sPES/PVP	0.65	-	-	0.1 NaCl	[38]
70% S-PVDF	SPVDF/PVDF	0.7	-	-	0.1 NaCl	[39]
MIL-10	sPES/MIL-101	1.04	85	-	0.1 NaCl	[40]
PM-5	PVC/St/DVB/SGO	1.76	82.3	-	0.085 NaCl	[41]
CEM-3	PAN/$PStSO_3Na$/PnBA	1.47	76.8	-	0.085 NaCl	[42]
S/P K30	sPES/PVP	0.54	80	90	0.86 NaCl	[43]
ClNH2	Cl-PES/NH_2-PES	2.2	-	93.8	0.05 NaCl	[44]
PES	PES	1.5	50	24	0.05 NaCl	(This work)
sPES	sPES	2.67	48	33	0.05 NaCl	(This work)

The sPES membrane, with an IEC of 2.67 meq/g, is among the highest reported, indicating excellent ion exchange capabilities essential for efficient ED. While some membranes show higher salt removal rates or current efficiency (CE), it is crucial to consider the feed solution concentration. Higher molarity feed solutions, as used in some studies, can artificially enhance performance metrics. This work uses a moderate feed solution concentration (0.05 mol/L NaCl), offering a more realistic performance assessment.

The PES membrane shows a salt removal rate of 24% and a CE of 50%, while the sPES membrane achieves a 33% salt removal rate and a CE of 48%. These results are significant, given the lower ionic strength of the feed solution, underscoring the membranes' effectiveness under practical conditions.

In summary, the developed PES and sPES membranes exhibit high IEC values and competitive performance metrics, demonstrating their potential for practical and scalable

ED applications. Their simple and cost-effective fabrication process further supports their industrial applicability.

4. Conclusions

The study of fabricated PES and sPES IEMs and their characterization analysis results are summarized below. Based on electrodialysis testing with PES membranes with different solvent evaporation times, the solvent evaporation time of 3 h was determined to be optimal based on several figures of merit (e.g., current density, current efficiency, salinity reduction, and normalized specific energy consumption), while the sPES membranes evaporated within 1 h show the best performance based on the same figures of merit. With electrodialysis test conditions of 3 cm/s flow velocity, 0.8 V/cell-pair, and 3 g/L NaCl feed water, for PES membranes, the average current density was 97 A/m^2, the current efficiency was 50%, the salinity reduction after 60 min of running was 24%, and the normalized specific energy consumption was approximately 0.045 $kWh/m^3/(meq/L)$. Under the same running conditions, for sPES membranes, the average current density was 130 A/m^2, the current efficiency was 48%, the salinity reduction after 60 min of running was 33%, and the normalized specific energy consumption was approximately 0.045 $kWh/m^3/(meq/L)$. In addition, the IEC of the sPES membrane is particularly notable at 2.67 meq/g, indicating superior ion exchange capacity. Generally, ED performance shows that the process of sulfonation increases the performance of salinity reduction from PES membranes to sPES membranes.

The increase in surface roughness from 0.996 nm for the PES membrane to 3.149 nm for the sPES membrane, as observed in AFM images, indicates the impact of the sulfonation process. This process increases the degree of sulfonation, which is further evidenced by the strengthened peaks in the FTIR-ATR and XPS spectra for the sPES membrane.

The developed PES and sPES membranes are highly effective for electrodialysis, especially in desalination and water purification. Their high IEC and competitive performance metrics make them suitable for large-scale industrial applications. New ion exchange membranes can significantly enhance the applicability, efficacy, and efficiency of ion removal processes in water treatment and resource recovery, especially with electrically driven separation processes, providing cost-effective and scalable solutions for improving water quality in various settings [45].

Author Contributions: Conceptualization, L.C., E.M.D. and W.S.W.; Methodology, L.C., E.M.D. and W.S.W.; Software, L.C.; Validation, L.C., E.M.D. and X.L.; Formal analysis, L.C.; Investigation, L.C.; Resources, E.M.D., X.L. and W.S.W.; Data curation, L.C.; Writing—original draft preparation, L.C.; Writing—review and editing, X.L. and W.S.W.; Visualization, L.C.; Supervision, X.L. and W.S.W.; Project administration, W.S.W.; Funding acquisition, X.L. and W.S.W. All authors have read and agreed to the published version of the manuscript.

Funding: This research was funded by the National Science Foundation through the Nanosystems Engineering Research Center (ERC) for Nanotechnology-Enabled Water Treatment (NEWT), grant number EEC-1449500. We would also like to acknowledge financial support from the U.S. NSF (IIP2122712 and CHE2216473), CPRIT(RP210165), NIH/NIAID (R41AI162477), and AAFS Lucas grants.

Institutional Review Board Statement: Not applicable.

Informed Consent Statement: Not applicable.

Data Availability Statement: The original contributions presented in this study are included in the article. Further inquiries can be directed to the corresponding author.

Conflicts of Interest: The authors declare no conflicts of interest.

References

1. Lim, Y.J.; Goh, K.; Goto, A.; Zhao, Y.; Wang, R. Uranium and lithium extraction from seawater: Challenges and opportunities for a sustainable energy future. *J. Mater. Chem. A* **2023**, *11*, 22551–22589. [CrossRef]
2. Latinis, A.; Papadopoulos, A.I.; Seferlis, P. Optimal Operational Profiles in an Electrodialysis Unit for Ion Recovery. *Chem. Eng. Trans.* **2021**, *88*, 1021–1026. [CrossRef]
3. Juve, J.M.A.; Christensen, F.M.S.; Wang, Y.; Wei, Z. Electrodialysis for metal removal and recovery: A review. *Chem. Eng. J.* **2022**, *435*, 134857. [CrossRef]
4. Biesheuvel, P.M.; Porada, S.; Elimelech, M.; Dykstra, J.E. Tutorial review of reverse osmosis and electrodialysis. *J. Membr. Sci.* **2022**, 647. [CrossRef]
5. da Trindade, L.G.; Zanchet, L.; Souza, J.C.; Leite, E.R.; Martini, E.M.A.; Pereira, E.C. Enhancement of sulfonated poly(ether ether ketone)-based proton exchange membranes doped with different ionic liquids cations. *Ionics* **2020**, *26*, 5661–5672. [CrossRef]
6. Solonchenko, K.; Kirichenko, A.; Kirichenko, K. Stability of Ion Exchange Membranes in Electrodialysis. *Membranes* **2023**, *13*, 52. [CrossRef]
7. Zhao, J.; Li, J.; Chen, Q.; Yang, M.; Li, Y.; Li, H.; Zhang, Y.; Wang, J. Fabrication of PVDF cation exchange membrane for electrodialysis: Influence and mechanism of crystallinity and leakage of co-ions. *J. Membr. Sci.* **2024**, *695*, 122389. [CrossRef]
8. Golubenko, D.V.; Van der Bruggen, B.; Yaroslavtsev, A.B. Ion exchange membranes based on radiation-induced grafted functionalized polystyrene for high-performance reverse electrodialysis. *J. Power Sources* **2021**, *511*, 230460. [CrossRef]
9. Wang, J.; Lim, J.; Wang, M.; Mi, B.; Miller, D.J.; McCloskey, B.D. Polyamide-Based Ion Exchange Membranes: Cation-Selective Transport through Water Purification Membranes. *ACS Appl. Polym. Mater.* **2024**, *6*, 2022–2030. [CrossRef]
10. Zhao, Y.; Qiu, Y.; Mai, Z.; Ortega, E.; Shen, J.; Gao, C.; Van der Bruggen, B. Symmetrically recombined nanofibers in a high-selectivity membrane for cation separation in high temperature and organic solvent. *J. Mater. Chem. A* **2019**, *7*, 20006–20012. [CrossRef]
11. Khan, M.I.; Zheng, C.; Mondal, A.N.; Hossain, M.; Wu, B.; Emmanuel, K.; Wu, L.; Xu, T. Preparation of anion exchange membranes from BPPO and dimethylethanolamine for electrodialysis. *Desalination* **2017**, *402*, 10–18. [CrossRef]
12. Gahlot, S.; Yadav, V.; Sharma, P.P.; Kulshrestha, V. Zn-MOF@SPES composite membranes: Synthesis, characterization and its electrochemical performance. *Sep. Sci. Technol.* **2019**, *54*, 377–385. [CrossRef]
13. He, S.; Lin, Y.; Ma, H.; Jia, H.; Liu, X.; Lin, J. Preparation of sulfonated poly(ether ether ketone) (SPEEK) membrane using ethanol/water mixed solvent. *Mater. Lett.* **2016**, *169*, 69–72. [CrossRef]
14. Wu, S.; Cheng, Y.; Ma, J.; Huang, Q.; Dong, Y.; Duan, J.; Mo, D.; Sun, Y.; Liu, J.; Yao, H. Preparation and ion separation properties of sub-nanoporous PES membrane with high chemical resistance. *J. Membr. Sci.* **2021**, *635*, 119467. [CrossRef]
15. Zhu, J.; Luo, B.; Qian, Y.; Sotto, A.; Gao, C.; Shen, J. Three-Dimensional Stable Cation-Exchange Membrane with Enhanced Mechanical, Electrochemical, and Antibacterial Performance by in Situ Synthesis of Silver Nanoparticles. *ACS Omega* **2019**, *4*, 16619–16628. [CrossRef] [PubMed]
16. Gahlot, S.; Sharma, P.P.; Gupta, H.; Kulshrestha, V.; Jha, P.K. Preparation of graphene oxide nano-composite ion-exchange membranes for desalination application. *RSC Adv.* **2014**, *4*, 24662–24670. [CrossRef]
17. Fan, H.; Xu, Y.; Zhao, F.; Chen, Q.B.; Wang, D.; Wang, J. A novel porous asymmetric cation exchange membrane with thin selective layer for efficient electrodialysis desalination. *Chem. Eng. J.* **2023**, *472*, 144856. [CrossRef]
18. Kim, I.C.; Choi, J.G.; Tak, T.M. Sulfonated Polyethersulfone by Heterogeneous Method and Its Membrane Performances. *J. Appl. Polym. Sci.* **1999**, *74*, 2046–2205. [CrossRef]
19. Cao, X.; Tang, M.; Liu, F.; Nie, Y.; Zhao, C. Immobilization of silver nanoparticles onto sulfonated polyethersulfone membranes as antibacterial materials. *Colloids Surf. B Biointerfaces* **2010**, *81*, 555–562. [CrossRef] [PubMed]
20. Unnikrishnan, L.; Nayak, S.K.; Mohanty, S.; Sarkhel, G. Polyethersulfone membranes: The effect of sulfonation on the properties. *Polym.—Plast. Technol. Eng.* **2010**, *49*, 1419–1427. [CrossRef]
21. Tavangar, T.; Ashtiani, F.Z.; Karimi, M. Morphological and performance evaluation of highly sulfonated polyethersulfone/polyethersulfone membrane for oil/water separation. *J. Polym. Res.* **2020**, *27*, 252. [CrossRef]
22. Guan, R.; Zou, H.; Lu, D.; Gong, C.; Liu, Y. Polyethersulfone sulfonated by chlorosulfonic acid and its membrane characteristics. *Eur. Polym. J.* **2005**, *41*, 1554–1560. [CrossRef]
23. Klaysom, C.; Ladewig, B.P.; Lu, G.Q.M.; Wang, L. Preparation and characterization of sulfonated polyethersulfone for cation-exchange membranes. *J. Membr. Sci.* **2011**, *368*, 48–53. [CrossRef]
24. Li, Z.; Ma, Z.; Xu, Y.; Wang, X.; Sun, Y.; Wang, R.; Wang, J.; Gao, X.; Gao, J. Developing homogeneous ion exchange membranes derived from sulfonated polyethersulfone/N-phthaloyl-chitosan for improved hydrophilic and controllable porosity. *Korean J. Chem. Eng.* **2018**, *35*, 1716–1725. [CrossRef]
25. Klaysom, C.; Moon, S.H.; Ladewig, B.P.; Lu, G.Q.M.; Wang, L. Preparation of porous ion-exchange membranes (IEMs) and their characterizations. *J. Membr. Sci.* **2011**, *371*, 37–44. [CrossRef]

26. Hyder, A.G.; Morales, B.A.; Cappelle, M.A.; Percival, S.J.; Small, L.J.; Spoerke, E.D.; Rempe, S.B.; Walker, W.S. Evaluation of electrodialysis desalination performance of novel bioinspired and conventional ion exchange membranes with sodium chloride feed solutions. *Membranes* **2021**, *11*, 217. [CrossRef]
27. Stenina, I.; Golubenko, D.; Nikonenko, V.; Yaroslavtsev, A. Selectivity of transport processes in ion-exchange membranes: Relationship with the structure and methods for its improvement. *Int. J. Mol. Sci.* **2020**, *21*, 5517. [CrossRef] [PubMed]
28. Wang, R.; Lin, S. Membrane Design Principles for Ion-Selective Electrodialysis: An Analysis for Li/Mg Separation. *Environ. Sci. Technol.* **2024**, *58*, 3552–3563. [CrossRef]
29. Jacob, K.N.; Kumar, S.S.; Thanigaivelan, A.; Tarun, M.; Mohan, D. Sulfonated polyethersulfone-based membranes for metal ion removal via a hybrid process. *J. Mater. Sci.* **2014**, *49*, 114–122. [CrossRef]
30. Rahimpour, A.; Madaeni, S.S.; Ghorbani, S.; Shockravi, A.; Mansourpanah, Y. The influence of sulfonated polyethersulfone (SPES) on surface nano-morphology and performance of polyethersulfone (PES) membrane. *Appl. Surf. Sci.* **2010**, *256*, 1825–1831. [CrossRef]
31. Zhao, J.; Sun, L.; Chen, Q.; Lu, H.; Wang, J. Modification of cation exchange membranes with conductive polyaniline for electrodialysis applications. *J. Membr. Sci.* **2019**, *582*, 211–223. [CrossRef]
32. Pal, S.; Mondal, R.; Guha, S.; Chatterjee, U.; Jewrajka, S.K. Homogeneous phase crosslinked poly(acrylonitrile-co-2-acrylamido-2-methyl-1-propanesulfonic acid) conetwork cation exchange membranes showing high electrochemical properties and electrodialysis performance. *Polymer* **2019**, *180*, 121680. [CrossRef]
33. Zhu, J.; Liao, J.; Jin, W.; Luo, B.; Shen, P.; Sotto, A.; Shen, J.; Gao, C. Effect of functionality of cross-linker on sulphonated polysulfone cation exchange membranes for electrodialysis. *React. Funct. Polym.* **2019**, *138*, 104–113. [CrossRef]
34. Thakur, A.K.; Pandey, R.P.; Shahi, V.K. Preparation, characterization and thermal degradation studies of bi-functional cation-exchange membranes. *Desalination* **2015**, *367*, 206–215. [CrossRef]
35. Shukla, G.; Pandey, R.P.; Shahi, V.K. Temperature resistant phosphorylated graphene oxide-sulphonated polyimide composite cation exchange membrane for water desalination with improved performance. *J. Membr. Sci.* **2016**, *520*, 972–982. [CrossRef]
36. Chen, S.; Wang, H.; Zhang, J.; Lu, S.; Xiang, Y. Effect of side chain on the electrochemical performance of poly (ether ether ketone) based anion-exchange membrane: A molecular dynamics study. *J. Membr. Sci.* **2020**, *605*, 118105. [CrossRef]
37. Zhao, J.; Guo, L.; Wang, J. Synthesis of cation exchange membranes based on sulfonated polyether sulfone with different sulfonation degrees. *J. Membr. Sci.* **2018**, *563*, 957–968. [CrossRef]
38. Sharma, P.P.; Yadav, V.; Rajput, A.; Kulshrestha, V. Synthesis of Chloride-Free Potash Fertilized by Ionic Metathesis Using Four-Compartment Electrodialysis Salt Engineering. *ACS Omega* **2018**, *3*, 6895–6902. [CrossRef] [PubMed]
39. Sharma, P.P.; Gahlot, S.; Kulshrestha, V. One Pot Synthesis of PVDF Based Copolymer Proton Conducting Membrane by Free Radical Polymerization for Electro-Chemical Energy Applications. *Colloids Surfaces A Physicochem. Eng. Asp.* **2017**, *520*, 239–245. [CrossRef]
40. Sharma, P.; Shahi, V.K. Assembly of MIL-101(Cr)-sulphonated poly(ether sulfone) membrane matrix for selective electrodialytic separation of Pb2+ from mono-/bi-valent ions. *Chem. Eng. J.* **2020**, *382*, 122688. [CrossRef]
41. Sharma, P.P.; Gahlot, S.; Rajput, A.; Patidar, R.; Kulshrestha, V. Efficient and Cost Effective Way for the Conversion of Potassium Nitrate from Potassium Chloride Using Electrodialysis. *ACS Sustain. Chem. Eng.* **2016**, *4*, 3220–3227. [CrossRef]
42. Pismenskaya, N.D.; Pokhidnia, E.V.; Pourcelly, G.; Nikonenko, V.V. Can the electrochemical performance of heterogeneous ion-exchange membranes be better than that of homogeneous membranes? *J. Membr. Sci.* **2018**, *566*, 54–68. [CrossRef]
43. Zhao, J.; Ren, L.; Chen, Q.B.; Li, P.; Wang, J. Fabrication of cation exchange membrane with excellent stabilities for electrodialysis: A study of effective sulfonation degree in ion transport mechanism. *J. Membr. Sci.* **2020**, *615*, 118539. [CrossRef]
44. Mabrouk, W.; Lafi, R.; Fauvarque, J.F.; Hafiane, A.; Sollogoub, C. New ion exchange membrane derived from sulfochlorated polyether sulfone for electrodialysis desalination of brackish water. *Polym. Adv. Technol.* **2021**, *32*, 304–314. [CrossRef]
45. Deemer, E.M.; Xu, P.; Verduzco, R.; Walker, W.S. Challenges and opportunities for electro-driven desalination processes in sustainable applications. *Curr. Opin. Chem. Eng.* **2023**, *42*, 100972. [CrossRef]